



Performance Analysis of cooperative SWIPT System: Intelligent Reflecting Surface versus Decode-and-Forward

H. Masoumi¹, M.J. Emadi²

¹ Department of Electrical Engineering, Amirkabir University of Technology, Tehran, Iran

ABSTRACT: In this paper, we explore the impacts of utilizing intelligent reflecting surfaces (IRS) in a power-splitting based simultaneous wireless information and power transfer (PS-SWIPT) system and compare its performance with the traditional decode and forward relaying system. To analyze a more practical system, it is also assumed that the receiving nodes are subject to decoding cost, and they are only informed about the imperfect channel state information (CSI). First, we drive the achievable data rate of single IRS-assisted cooperative communications, and to maximize the achievable rate, optimal phase shifts for each elements of the IRS node is derived, and finally the optimal power splitting ratio at the destination is obtained. The system model is extended to consider two and multiple IRS-assisted system. The respective achievable rates are derived and optimized accordingly. To evaluate the benefits of using the IRS, we have also derived the achievable rate for a two-hop decode and forward relaying scheme, wherein both the relay and the destination not only did they equip with pre-dedicated power but also they can harvest energy from the received signals to provide the required power for the decoding. For this case, optimal power splitting factor at both the relay and the destination are optimized. Finally, the numerical results are presented to examine and compare the performance of the two considered systems. It is shown that by increasing the size of the reflecting surface, IRS-based cooperative transmission outperforms the conventional relaying scheme.

Review History:

Received: 2019-06-22
Revised: 9/15/2019
Accepted: 2019-09-17
Available Online: 2019-12-01

Keywords:

Intelligent reflecting surface
power-splitting SWIPT system
decoding cost
decode-and-forward relaying
imperfect CSI

1. Introduction

Next wireless communication systems must be designed in a way to support various use cases; Enhanced broadband communications, massive machine type communications, and ultra-reliable and low latency communications. To support such different services, various key enabling technologies such as massive multiple-input and multiple-output (mMIMO), full-duplex radio, cooperative transmissions, device-to-device communications, small-cell and millimeter wave techniques are developed to provide reliable communications and increase the area throughput up to 1000-fold [1]. On the other hand, to control the development costs of the network and devices, using low-cost devices along with green communications techniques has gained research interests to have a cost-efficient communications network [1-4].

One of the novel promising and cost-efficient scheme beyond the mMIMO system, to improve spectral- and energy-efficiency, is to utilize the intelligent reflecting surfaces (IRS) to constructively control the channel environment [2-5]. The IRS includes number of low-cost passive reconfigurable reflective metamaterial elements which can reflect the incident radio frequency signals toward a desired user or make a null toward a spatial direction. Recently, the IRS has gained many research interests due to its different applications, e.g. providing non-

line of sight communications when the direct link is blocked, the coverage extension of the network, enhancing the secrecy rate, enabling more efficient wireless power transfer to the energy harvesting node, and spatial modulation [2-6], and interestingly these benefits are because of controlling phase of each elements while consuming low power at IRS [5, 7, 8].

It is worth noting that in the conventional digital communication systems introduced by Claude E. Shannon [9], it is assumed that the channel is random and to utilize the capacity of the channel, one needs to adapt the transmission and reception schemes. While in IRS system not only one can optimize the transceiver algorithms, but also can dynamically reconfigure the channel environment to improve information transfer. Thus, the principle of IRS open doors to revisit the fundamental modeling and analyzing of the communication systems from theoretical to practical points of view [10]. In [11], energy efficiency of a multi user IRS-assisted downlink transmission of a mMIMO base station is analyzed which outperforms that of the conventional multi-antenna amplify-and-forward (AF) relaying. Effects of hardware impairments on the capacity degradation of the RIS-based communication systems is analyzed in [12]. Energy- and spectral-efficiency of a single-user communication systems is compared for the decode-and-forward (DF) relaying scheme and the RIS-based transmission [13]. It is shown that the large IRS-based scheme



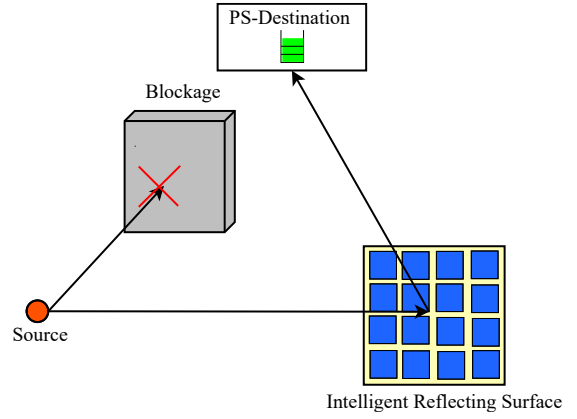
outperforms the DF-relaying one. Instead of assuming continuous phase shifts at each element of RIS, beamforming optimization of a multi-user downlink data transmission in presence of discrete phase shifters is analyzed in [14].

On the other hand, to increase energy efficiency of the system, energy harvesting (EH) and wireless power transfer has attracted research interests. In a simultaneous wireless information and power (SWIPT)-enabled system, each EH node can adaptively manage its received signal for both EH and or information decoding (ID) [15]. For cooperative communication systems with SWIPT capabilities many researches have conducted from different perspective; Optimal power splitting (PS)-SWIPT schemes for a two-way DF, and full-duplex DF relaying strategies are analyzed in [16] and [17], respectively. Two-way massive multi-antenna relay channel wherein users are capable of harvesting energy via power splitting for data transmission is studied in [18]. For an AF SWIPT relaying over Nakagami- m channels bit error rate of the system is derived in [19]. In [20], SWIPT two-way AF relay network is considered to maximize the secrecy sum-rate subject to attaining minimum energy requirement at the EH node. Besides, in contrary to the conventional communication system, at the low-power EH nodes, power consumption for ID, named as *decoding cost*, may become non-negligible. For internet of things (IoT) with SWIPT-enabled nodes, the energy efficiency subject to *constant* circuit power consumption is investigated in [21, 22]. Moreover, optimal power management for EH wireless networks with decoding cost are studied in [23-25], wherein the decoding cost function is assumed to be an *increasing convex function* of the data rate which simplifies the optimization problems. Finally, for point-to-point and relay channels with SWIPT-enabled nodes and *perfect* channel state information, the optimal data rate with general non-decreasing decoding cost function analytically is derived in [26].

To the best of our knowledge, the performance of the state-of-the-art IRS and SWIPT-enabled cooperative communication systems has not been studied in the literature. In this paper, it is assumed that *imperfect CSI* is available, and the nodes wherein information is decoded are subject to *decoding cost*. Moreover, the performance of the IRS-enabled system is compared with that of the classical decode-and-forward relaying scheme. The main contribution of this paper are as follows

- Deriving achievable rate of a SWIPT-enabled IRS system with decoding cost and imperfect CSI.
- Achievable rate analysis of the SWIPT-enabled DF relay with decoding cost and imperfect CSI.
- Presenting closed-form expressions for optimal end-to-end data rate of the two systems by adjusting power splitting ratios.
- Extending the results for multiple-IRS scenario.
- Presenting numerical results to evaluate and compare the performance of the proposed systems.

The organization of the paper is as follows. Section 2 presents the IRS- and relay-based system models. Achievable rates and performance analysis are derived and analyzed in



(a) IRS-assisted cooperative SWIPT system

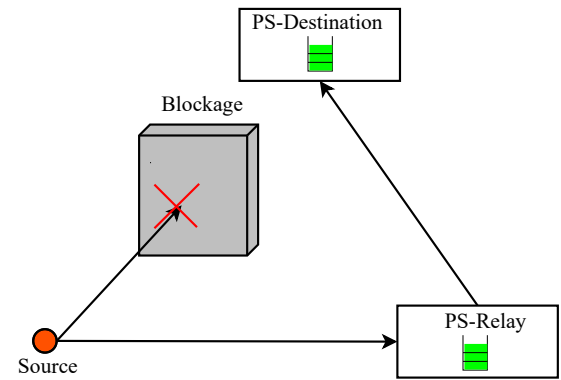


Fig. 1. Cooperative SWIPT systems. (a) IRS-assisted, (b) Relay-assisted.

Section 3. Numerical results are discussed in Section 4, and the paper is concluded in Section 5.

2. System Model

To investigate the advantages of IRS-enabled wireless system over other conventional cooperative techniques, this paper considers decode-and-forward relaying as a baseline. Hence, we consider single-antenna source and destination nodes where the line-of-sight (LOS) path has been blocked; however, they can communicate via an assisting IRS/relay node which has a LOS path with the source and destination. The system model is depicted in Fig. 1. Moreover, the channel between each pair of nodes is assumed to be a Rayleigh flat-fading one.

2-1- IRS-assisted transmission

Assume an IRS with N reflecting elements to cooperate in transferring information from the source to the destination. The channels between source-IRS and IRS-destination are respectively denoted by $\mathbf{g}_{sr} = \sqrt{\beta_{sr}}\mathbf{h}_{sr}$ and $\mathbf{g}_{rd} = \sqrt{\beta_{rd}}\mathbf{h}_{rd}$ which are $N \times 1$ vectors, wherein β_{sr} and β_{rd} represent the path-losses while \mathbf{h}_{sr} and \mathbf{h}_{rd} indicate the small-scale fading which are distributed according to a circularly symmetric complex Gaussian (CSCG) zero-mean and unit-variance random

variables. The reflection properties of the IRS is denoted by the following diagonal matrix

$$\Theta = \alpha \times \text{diag} \left[e^{j\theta_1}, \dots, e^{j\theta_N} \right] \quad (1)$$

where $\theta_1, \dots, \theta_N$ are phase-shift variables that one can optimize them to improve the performance of the system and $\alpha \in (0,1]$ is a fixed amplitude reflection coefficient [8]. Thus, the received signal at the destination is given by

$$y = \mathbf{g}_{sr}^H \Theta \mathbf{g}_{rd} \sqrt{p} \times s + n_d \quad (2)$$

where p is the transmit power, $s \sim CN(0,1)$ is the information symbol and $n_d \sim CN(0, N_d)$ is the receiver noise. It is worth noting that for this scenario, the IRS only cooperatively reflects the received signal by adjusting phase-shift variables, and the destination performs decoding which is subject to the decoding cost at the destination. To charge the battery of the destination to support the consumed power due to the decoding cost, the destination employs power splitting technique to harvest energy for the information decoding. Therefore, the splitted received signal for energy harvesting, y_{EH} , and information decoding, y_{ID} , are as follows

$$y_{EH} = \sqrt{\rho} y, \quad y_{ID} = \sqrt{1-\rho} y + n_p \quad (3)$$

where $\rho \in [0,1]$ is the power splitting ratio and $n_p \sim CN(0, N_p)$ denotes the processing noise at the destination. The decoding cost function at the destination is modeled by an exponential function of the decodable rate, i.e. $\varphi(R) = \xi(2^R - 1)$ [23].

2-2- Relay-assisted transmission

In this scenario, we consider a fading two-hop DF relay channel where the relay and the destination employ adaptive power splitting to partly harvest energy from their received signals. The relay uses this energy for decoding and retransmitting of the information. Also, the destination harvests some portion of the received signal for decoding the information. Therefore, the relay and the destination have to select optimal splitting ratios such that the end-to-end achievable rate is maximized. The received signals at the relay and the destination are respectively given by

$$y_r = \mathbf{g}_{sr} \sqrt{p} \times s + n_r \quad (4)$$

$$y_d = \mathbf{g}_{rd} \sqrt{p_r} \times s_r + n_d \quad (5)$$

where $n_r \sim CN(0, N_r)$ and $n_d \sim CN(0, N_d)$ denote the receiver noise at the relay and the destination, respectively. Moreover, $s_r \sim CN(0,1)$ and p_r represent the information symbol retransmitted by the relay and the corresponding transmit power, respectively. Similar to equation (3) the splitted signals for EH and ID at the relay and the destination are given by

$$y_{EH_i} = \sqrt{\rho_i} y_i, \quad y_{ID_i} = \sqrt{1-\rho_i} y_i + n_{p,i} \quad (6)$$

where $i \in \{r, d\}$ represents the relay and the destination. Therefore, $\rho_r, \rho_d \in [0,1]$ indicate the power splitting ratio and $n_{p,r} \sim CN(0, N_{p,r}), n_{p,d} \sim CN(0, N_{p,d})$ account for the processing noise at the relay and the destination. Finally, the decoding cost functions at the relay and the destination are defined as $\varphi_i(R) = \xi_i(2^R - 1)$.

3- Performance Analysis with Imperfect CSI

In this section, performance of the considered systems in terms of the achievable rate are analyzed and optimized to improve the performance of the systems.

3-1- IRS-assisted transmission

Here, we first explore the results for a single-IRS case, then we extend the results for the two-ISR scenario and multiple-IRS cooperative system.

3-1-1 Single-IRS scenario

In this section, the achievable data rate of the system is derived, and then optimal power-splitting ratio is obtained.

Achievable data rate

Based on equations (1-3) the harvested power at the destination is given by

$$\begin{aligned} P_{EH} &= \eta E \left\{ |y_{EH}|^2 \right\} = \\ &= \eta E \left\{ \left| \sqrt{\rho} \left(\mathbf{g}_{sr}^H \Theta \mathbf{g}_{rd} \sqrt{p} \times s + n \right) \right|^2 \right\} = \\ &= \eta \rho \left[\alpha^2 p E \left\{ \left| s \times \sum_{l=1}^N \mathbf{g}_{sr}^* [l] \mathbf{g}_{rd} [l] e^{j\theta_l} \right|^2 \right\} \right. \\ &\quad \left. + E \left\{ |n|^2 \right\} \right] \quad (7) \\ &= \eta \rho \left[\alpha^2 p E \left\{ |s|^2 \right\} E \left\{ \sum_{l=1}^N \left| \mathbf{g}_{sr}^* [l] \mathbf{g}_{rd} [l] e^{j\theta_l} \right|^2 \right\} + \right. \\ &\quad \left. E \left\{ |n|^2 \right\} \right] = \\ &= \eta \rho \left[\alpha^2 p N \beta_{sr} \beta_{rd} + N \right], \end{aligned}$$

where $\eta \in [0,1]$ denotes the energy conversion efficiency. Furthermore, for computing the achievable rate with imperfect CSI one can assume that $\mathbf{g}_{sr} = \hat{\mathbf{g}}_{sr} + \mathbf{e}_{sr}$ and $\mathbf{g}_{rd} = \hat{\mathbf{g}}_{rd} + \mathbf{e}_{rd}$, where $\hat{\mathbf{g}}_{sr} \sim CN(0, (\beta_{sr} - N_{sr}) \mathbf{I}_{N \times N}), \hat{\mathbf{g}}_{rd} \sim CN(0, (\beta_{rd} - N_{rd}) \mathbf{I}_{N \times N})$ and it is assumed that they are the minimum mean square error estimations of $\mathbf{g}_{sr}, \mathbf{g}_{rd}$ and $\mathbf{e}_{sr} \sim CN(0, N_{sr} \mathbf{I}_{N \times N}), \mathbf{e}_{rd} \sim CN(0, N_{rd} \mathbf{I}_{N \times N})$ represent the corresponding estimation errors which are independent of the estimated channels. Thus, the received signal for information decoding in (3) can be rewritten as follows

$$y_{ID} = \sqrt{1-\rho} \left((\hat{\mathbf{g}}_{sr} + \mathbf{e}_{sr})^H \Theta (\hat{\mathbf{g}}_{rd} + \mathbf{e}_{rd}) \sqrt{p \times s + n} \right) + n_p = \sqrt{1-\rho} \hat{\mathbf{g}}_{sr}^H \Theta \hat{\mathbf{g}}_{rd} \sqrt{p \times s} + \underbrace{\sqrt{1-\rho} (\hat{\mathbf{g}}_{sr}^H \Theta \mathbf{e}_{rd} + \mathbf{e}_{sr}^H \Theta \hat{\mathbf{g}}_{rd} + \mathbf{e}_{sr}^H \Theta \mathbf{e}_{rd})}_{n_{eq}} \sqrt{p \times s} + \sqrt{1-\rho} n + n_p \quad (8)$$

Theorem 1. The achievable rate of the IRS-assisted system with imperfect CSI is given by

$$R_{IRS} = \max_{\theta_1, \dots, \theta_N} \log_2 \left(1 + \frac{(1-\rho) p \left| \hat{\mathbf{g}}_{sr}^H \Theta \hat{\mathbf{g}}_{rd} \right|^2}{E \left\{ n_{eq}^2 \right\}} \right) \quad (9)$$

$$= \log_2 \left(1 + \frac{\alpha^2 (1-\rho) p \left| \sum_{l=1}^N \hat{\mathbf{g}}_{sr} [l] \hat{\mathbf{g}}_{rd} [l] \right|^2}{(1-\rho) \left[\alpha^2 p N \left(\frac{\beta_{sr} N_{rd} + \beta_{rd} N_{sr} + N_{sr} N_{rd}}{N_{sr} N_{rd}} \right) + N_d \right] + N_p} \right)$$

Proof: For the received signal in equation (8), the data rate can be written in the form of the first line of equation in (9). Moreover, since $\hat{\mathbf{g}}_{sr}^H \Theta \hat{\mathbf{g}}_{rd} = \sum_{l=1}^N \hat{g}_{sr}^* [l] \hat{g}_{rd} [l] e^{j\theta_l}$, the values of the phase-shift variables which maximize this summation and the data rate is $\theta_l = -\arg \left(\hat{g}_{sr}^* [l] \hat{g}_{rd} [l] \right), \forall l$. It can be proved that by following the same steps provided in [8]. Additionally, the denominator of the rate, i.e. $E \left\{ n_{eq}^2 \right\}$, which becomes independent of the values of the phase-shift variables is given by

$$E \left\{ n_{eq}^2 \right\} = (1-\rho) \left[\begin{aligned} & p E \left\{ \left| \hat{\mathbf{g}}_{sr}^H \Theta \mathbf{e}_{rd} \right|^2 \right\} + \\ & p E \left\{ \left| \mathbf{e}_{sr}^H \Theta \hat{\mathbf{g}}_{rd} \right|^2 \right\} + \\ & p E \left\{ \left| \mathbf{e}_{sr}^H \Theta \mathbf{e}_{rd} \right|^2 \right\} + E \left\{ n_d^2 \right\} \end{aligned} \right] + E \left\{ n_p^2 \right\} =$$

$$(1-\rho) \left[\begin{aligned} & p \alpha^2 N \beta_{sr} (\beta_{rd} - N_{rd}) + \\ & p \alpha^2 N (\beta_{sr} - N_{sr}) \beta_{rd} + \\ & p \alpha^2 N (\beta_{sr} - N_{sr}) (\beta_{rd} - N_{rd}) + N_d \end{aligned} \right] + N_p =$$

$$(1-\rho) \left[\alpha^2 p N (\beta_{sr} N_{rd} + \beta_{rd} N_{sr} + N_{sr} N_{rd}) + N_d \right] + N_p.$$

Note that in the above equation we have used the following result,

$$E \left\{ \left| \hat{\mathbf{g}}_{sr}^H \Theta \mathbf{e}_{rd} \right|^2 \right\} = \alpha^2 E \left\{ \left| \sum_{l=1}^N \hat{g}_{sr}^* [l] e_{rd} [l] e^{j\theta_l} \right|^2 \right\} =$$

$$\alpha^2 E \left\{ \sum_{l=1}^N \sum_{k=1}^N \hat{g}_{sr}^* [l] \hat{g}_{sr} [k] e_{rd} [l] e_{rd}^* [k] e^{j\theta_l} e^{-j\theta_k} \right\}$$

$$= \alpha^2 E \left\{ \sum_{l=1}^N \left| \hat{g}_{sr} [l] \right|^2 \left| e_{rd} [l] \right|^2 \right\} +$$

$$\alpha^2 E \left\{ \sum_{l=1}^N \sum_{k \neq l}^N \hat{g}_{sr}^* [l] \hat{g}_{sr} [k] e_{rd} [l] e_{rd}^* [k] e^{j\theta_l} e^{-j\theta_k} \right\} \quad (10)$$

$$= \alpha^2 \sum_{l=1}^N E \left\{ \left| \hat{g}_{sr} [l] \right|^2 \right\} E \left\{ \left| e_{rd} [l] \right|^2 \right\} +$$

$$\alpha^2 \sum_{l=1}^N \sum_{k \neq l}^N \underbrace{E \left\{ \hat{g}_{sr}^* [l] \hat{g}_{sr} [k] e_{rd} [l] e_{rd}^* [k] \right\}}_{(a) = 0} e^{j\theta_l} e^{-j\theta_k}$$

$$= \alpha^2 \sum_{l=1}^N \beta_{sr} (\beta_{sr} - N_{sr}) = \alpha^2 N \beta_{sr} (\beta_{sr} - N_{sr}),$$

where (a) is due to the fact that $\hat{g}_{sr}^* [l], \hat{g}_{sr} [k], e_{rd} [l]$ and

$e_{rd}^* [k]$ are independent and zero-mean random variables. Also, one can evaluate the other two terms in a similar way.

Optimization problem

The data rate maximization problem is formulated as follows

$$P_1 = \begin{cases} \text{maximize} & R_t \\ \text{subject to} & R_t = \min(R_{IRS}, R_\phi), \end{cases} \quad (11)$$

where R_{IRS} is the data rate of the system given in equation (9), and R_ϕ represents the decodable rate at the destination which is given by

$$R_\phi = \phi^{-1} (P_{EH} + P^0). \quad (12)$$

and P^0 indicates the *inherent power* available at the destination.

Theorem 2. One can obtain the optimal data rate for a single-IRS assisted system as follows

$$R_t^* = \min \left(\Upsilon(\Omega^{-1}(a)), \Upsilon(0) \right), \quad (13)$$

where

$$\Omega(x) = \frac{1}{\eta x} (\phi(\Upsilon(x)) - P^0), \quad \Upsilon(x) =$$

$$\log_2 \left(1 + \frac{\alpha^2 (1-x) p \left| \sum_{l=1}^N \hat{\mathbf{g}}_{sr} [l] \hat{\mathbf{g}}_{rd} [l] \right|^2}{(1-x) \left[\alpha^2 p N \left(\frac{\beta_{sr} N_{rd} + \beta_{rd} N_{sr} + N_{sr} N_{rd}}{N_{sr} N_{rd}} \right) + N_d \right] + N_p} \right),$$

$$a = \alpha^2 p \left[\sum_{l=1}^N \left| \hat{\mathbf{g}}_{sr} [l] \hat{\mathbf{g}}_{rd} [l] \right|^2 + N (\beta_{sr} N_{rd} + \beta_{rd} N_{sr} + N_{sr} N_{rd}) + N_d \right]$$

Sketch of proof: Since R_{IRS} in equation (9) is decreasing function of ρ and R_ϕ is an increasing function of ρ , similar to the proof of Theorem 1 in [26] the optimum rate obtains from the intersection of R_{IRS} and R_ϕ .

Remark 1. When the value of the inherent power is larger than $P^0 \geq \Omega(\Upsilon(0))$, the destination has enough power for decoding the received signal and therefore it does not need to harvest energy. In this case the optimum data rate is $R_t^* = \Upsilon(0)$.

3-1-2 Two-IRS scenario

Herein, we extend the results to the case where two distend and physically separated IRSs contribute to the transmission. For this setup the received signal at the destination is given by

$$y = \left(\mathbf{g}_{sr1}^H \Theta_1 \mathbf{g}_{rd1} + \mathbf{g}_{sr2}^H \Theta_2 \mathbf{g}_{rd2} \right) \sqrt{p} \times s + n, \quad (14)$$

where $\Theta_m = \alpha_m \times \text{diag} \left[\left[e^{j\theta_1^m}, \dots, e^{j\theta_{N_m}^m} \right] \right]$ denotes $N_m \times N_m$ diagonal matrix of the phase-shift variables for the two IRSs and $\mathbf{g}_{srm}, \mathbf{g}_{rdm}$ represent $N_m \times 1$ vector of the channels between the source-IRS and IRS-destination, respectively. Moreover, $m \in \{1, 2\}$ indicates the two different IRSs. Similar to what is developed in case of the single-IRS scenario with imperfect CSI, one can account for the imperfection of the CSI by replacing $\mathbf{g}_{srm} = \hat{\mathbf{g}}_{srm} + \mathbf{e}_{srm}, \mathbf{g}_{rdm} = \hat{\mathbf{g}}_{rdm} + \mathbf{e}_{rdm}$ and therefore the received signal for information decoding can be rewritten in the following form

$$y_{ID} = \sqrt{1-\rho} \left(\hat{\mathbf{g}}_{sr1}^H \Theta_1 \hat{\mathbf{g}}_{rd1} + \hat{\mathbf{g}}_{sr2}^H \Theta_2 \hat{\mathbf{g}}_{rd2} \right) \sqrt{p} \times s + \underbrace{\sqrt{1-\rho} \left[\left(\hat{\mathbf{g}}_{sr1}^H \Theta_1 \mathbf{e}_{rd1} + \mathbf{e}_{sr1}^H \Theta_1 \hat{\mathbf{g}}_{rd1} + \mathbf{e}_{sr1}^H \Theta_1 \mathbf{e}_{rd1} + \hat{\mathbf{g}}_{sr1}^H \Theta_1 \mathbf{e}_{rd1} + \mathbf{e}_{sr1}^H \Theta_1 \hat{\mathbf{g}}_{rd1} + \mathbf{e}_{sr1}^H \Theta_1 \mathbf{e}_{rd1} \right) \right]}_{n_{eq}} \sqrt{p} \times s + n + n_p. \quad (15)$$

Theorem 3. The achievable rate of the two-IRS-assisted system with imperfect CSI is given by

$$R_{2-IRS} = \max_{\substack{\theta_1^1, \dots, \theta_{N_1}^1 \\ \theta_1^2, \dots, \theta_{N_2}^2 \\ \vdots \\ \theta_1^M, \dots, \theta_{N_M}^M}} \log_2 \left(1 + \frac{(1-\rho)p \left| \hat{\mathbf{g}}_{sr1}^H \Theta_1 \hat{\mathbf{g}}_{rd1} + \hat{\mathbf{g}}_{sr2}^H \Theta_2 \hat{\mathbf{g}}_{rd2} \right|^2}{E \left\{ |n_{eq}|^2 \right\}} \right) = \log_2 \left(1 + \frac{(1-\rho)p \left[\alpha_1 \sum_{l=1}^N \left| \hat{\mathbf{g}}_{sr1} [l] \right| \left| \hat{\mathbf{g}}_{rd1} [l] \right| + \alpha_2 \sum_{l=1}^N \left| \hat{\mathbf{g}}_{sr2} [l] \right| \left| \hat{\mathbf{g}}_{rd2} [l] \right| \right]^2}{(1-\rho) p \left[\left(\alpha_1^2 N_1 \begin{pmatrix} \beta_{sr1} N_{rd1} + \\ \beta_{rd1} N_{sr1} - \\ N_{sr1} N_{rd1} \end{pmatrix} + N_d + N_p \right) + \alpha_2^2 N_2 \begin{pmatrix} \beta_{sr2} N_{rd2} + \\ \beta_{rd2} N_{sr2} - \\ N_{sr2} N_{rd2} \end{pmatrix} \right]} \right). \quad (16)$$

Proof: To find the optimal values of the phase-shift, we first note that similar to Theorem 1, $E \left\{ |n_{eq}|^2 \right\}$ is computed and is independent of the phase-shifts. Moreover, the numerator of the signal to noise and interference ratio can be reformulated as follows

$$\hat{\mathbf{g}}_{sr1}^H \Theta_1 \hat{\mathbf{g}}_{rd1} + \hat{\mathbf{g}}_{sr2}^H \Theta_2 \hat{\mathbf{g}}_{rd2} = \hat{\mathbf{G}}_{sr}^H \Theta \hat{\mathbf{G}}_{rd},$$

$$\hat{\mathbf{G}}_{sr} = \begin{bmatrix} \alpha_1 \hat{\mathbf{g}}_{sr1} \\ \alpha_2 \hat{\mathbf{g}}_{sr2} \end{bmatrix}, \quad \Theta = \begin{bmatrix} \frac{1}{\alpha_1} \Theta_1 & 0_{N_1 \times N_2} \\ 0_{N_2 \times N_1} & \frac{1}{\alpha_2} \Theta_2 \end{bmatrix}, \quad \hat{\mathbf{G}}_{rd} = \begin{bmatrix} \hat{\mathbf{g}}_{rd1} \\ \hat{\mathbf{g}}_{rd2} \end{bmatrix}.$$

Note that in above equation, we have transferred the

effects of the fixed amplitude reflection coefficients to the channel gain such that the matrix Θ only contains phase-shifts, i.e. $\theta = \text{diag} \left[\left[e^{j\theta_1^1}, \dots, e^{j\theta_{N_1}^1}, e^{j\theta_1^2}, \dots, e^{j\theta_{N_2}^2} \right] \right]$. Therefore, by following similar approach as in the case of the single-IRS scenario, the maximizing values of the phase-shifts obtain as follows

$$\theta_i^1 = -\arg \left(\hat{\mathbf{g}}_{sr1}^* [i] \hat{\mathbf{g}}_{rd1} [i] \right), \quad i \in \{1, \dots, N_1\};$$

$$\theta_i^2 = -\arg \left(\hat{\mathbf{g}}_{sr2}^* [i] \hat{\mathbf{g}}_{rd2} [i] \right), \quad i \in \{1, \dots, N_2\}.$$

The harvested energy in the case of 2-IRS scenario is given by

$$P_{EH} = \eta \rho E \left\{ \left| \left(\mathbf{g}_{sr1}^H \Theta_1 \mathbf{g}_{rd1} + \mathbf{g}_{sr2}^H \Theta_2 \mathbf{g}_{rd2} \right) \sqrt{p} s + n \right|^2 \right\} = \eta \rho \left[\left[\alpha_1^2 N_1 \beta_{sr1} \beta_{rd1} + \alpha_2^2 N_2 \beta_{sr2} \beta_{rd2} \right] p + N_d \right]. \quad (17)$$

Furthermore, maximum data rate that can be achieved by adjusting the power splitting ratio is obtained in the similar way that developed for the single-IRS scenario in Theorem 2.

Proposition 1. The achievable data rate of the multiple-IRS-assisted system with M separate IRSs where m th IRS equipped with N_m reflecting elements and with imperfect CSI is given by

$$R_{2-IRS} = \max_{\substack{\theta_1^1, \dots, \theta_{N_1}^1 \\ \vdots \\ \theta_1^M, \dots, \theta_{N_M}^M}} \log_2 \left(1 + \frac{(1-\rho)p \left| \sum_{m=1}^M \hat{\mathbf{g}}_{srm}^H \Theta_m \hat{\mathbf{g}}_{rdm} \right|^2}{E \left\{ |n_{eq}|^2 \right\}} \right) = \log_2 \left(1 + \frac{(1-\rho)p \left[\sum_{m=1}^M \alpha_m \sum_{l=1}^N \left| \hat{\mathbf{g}}_{srm} [l] \right| \left| \hat{\mathbf{g}}_{rdm} [l] \right| \right]^2}{(1-\rho) \left[N_d + p \sum_{m=1}^M N_m \alpha_m^2 (\beta_{srm} N_{rdm} + \beta_{rdm} N_{srm} - N_{srm} N_{rdm}) \right] + N_p} \right). \quad (18)$$

and the harvested energy is $P_{EH} = \eta \rho \left[N_d + p \sum_{m=1}^M \alpha_m^2 N_m \beta_{srm} \beta_{rdm} \right]$. Additionally, the optimizing values of power splitting ratio is obtained in the similar way as developed for single-IRS case in Theorem 2. Finally, the optimizing values of the phase-shifts are given by

$$\theta_i^m = -\arg \left(\hat{\mathbf{g}}_{srm}^* [i] \hat{\mathbf{g}}_{rdm} [i] \right), \quad i \in \{1, \dots, N_m\}, \quad m \in \{1, \dots, M\}. \quad (19)$$

Sketch of proof: Here, the received signal at the destination is in the form of $y = \left(\sum_{m=1}^M \mathbf{g}_{srm}^H \Theta_m \mathbf{g}_{rdm} \right) \sqrt{p} \times s + n$. Following similar approach as in case of the 2-IRS scenario, one can derive the results.

3-2- Relay-assisted transmission

Here, first the achievable data rate for a two-hop decode-and-forward relay SWIPT system with decoding cost at the relay and the destination is derived then optimization cost at the relay and the destination is proposed to maximize the end-to-end data rate by adjusting the power splitting ratios at the relay and the destination. It is worth noting that the relay and the destination have inherent powers and they are enabled with harvesting capability to

gather extra power to improve the performance.

For this system, based on the received signals at the relay and the destination given in (4), (5) and their corresponding split signals for information decoding and energy harvesting in (6) for imperfect channel state information one can rewrite the information decoding signals at the relay and the destination as follows

$$y_{ID_r} = \sqrt{1-\rho_r}y_r + n_{p,r} = \sqrt{1-\rho_r}\hat{g}_{sr}\sqrt{p}\times s + \sqrt{1-\rho_r}\left(e_{sr}\sqrt{p}\times s + n_r\right) + n_{p,r}, \quad (20)$$

$$y_{ID_d} = \sqrt{1-\rho_d}y_d + n_{p,d} = \sqrt{1-\rho_d}\hat{g}_{rd}\sqrt{p}\times s + \sqrt{1-\rho_d}\left(e_{rd}\sqrt{p}\times s + n_d\right) + n_{p,d}. \quad (21)$$

Moreover, the harvested power at the relay and the destination is given by

$$P_{EH_r} = \eta_r\rho_r\left[p\beta_{sr} + N_r\right], \quad (22)$$

$$P_{EH_d} = \eta_d\rho_d\left[p\beta_{rd} + N_d\right], \quad (23)$$

where $\eta_r, \eta_d \in [0,1]$ account for the energy conversion efficiencies at the relay and the destination. Therefore, the end-to-end data rate maximization problem is formulated as

$$P_2 = \begin{cases} \text{maximize} & R_t \\ \text{subject to} & R_t = \min(R_{sr}, R_{rd}, R_\phi), \end{cases} \quad (24)$$

where R_{sr}, R_{rd}, R_ϕ are the data rates for the source-relay and the relay-destination channels and the possible decodable rate at the destination (due to the decoding cost), respectively;

$$R_{sr} \leq \log_2\left(1 + \frac{(1-\rho_r)|\hat{g}_{sr}|^2 p}{(1-\rho_r)(pN_{sr} + N_r) + N_{p,r}}\right) = 2f_1(\rho_r), \quad (25)$$

$$R_{rd} \leq \log_2\left(1 + \frac{(1-\rho_d)|\hat{g}_{rd}|^2 P_r}{(1-\rho_d)(N_{rd}P_r + N_d) + N_{p,d}}\right) = 2f_2(\rho_r, \rho_d, R_t), \quad (26)$$

$$R_\phi \leq \varphi_d^{-1}(P_{EH_d} + P_d^0) = 2f_3(\rho_r, \rho_d, R_t), \quad (27)$$

where $p_r = P_{EH_r} - \varphi_r(R_t) + P_r^0$ in which P_r^0 and P_d^0 denote inherent powers at the relay and destination, respectively.

Theorem 4. The optimal achievable rate for the SWIPT-enabled decode-and-forward relay with decoding cost and imperfect CSI is given by

$$R_t^* = \frac{1}{2} \min\left(\Upsilon(\Omega_1^{-1}(a)), \Upsilon(\Omega_2^{-1}(a)), \Upsilon(0)\right), \quad (28)$$

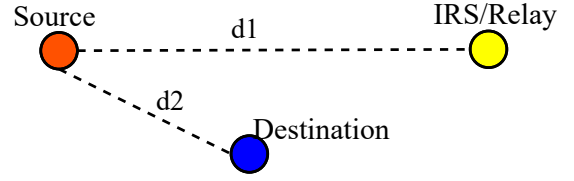


Fig. 2. The simulation setup.

where

$$\Omega_1(x) = \frac{1}{\eta_r x} \left[\frac{\varphi_d(\Upsilon(x)) - P_d^0}{\eta_d \psi(x) |\hat{g}_{rd}|^2} + \varphi_r \left(\frac{1}{2} \Upsilon(x) \right) - P_r^0 - \frac{N_d}{|\hat{g}_{rd}|^2} \right],$$

$$\Omega_2(x) = \frac{1}{\eta_r x} \left[\frac{(N_d + N_{p,d})(2^{\Upsilon(x)} - 1)}{|\hat{g}_{rd}|^2 - (2^{\Upsilon(x)} - 1)N_{rd}} + \varphi_r \left(\frac{1}{2} \Upsilon(x) \right) - P_r^0 \right], \quad (29)$$

$$\psi(x) = 1 - \left[\frac{|\hat{g}_{rd}|^2}{N_{p,d}} \left(\left(\eta_r x a - \varphi_r \left(\frac{1}{2} \Upsilon(x) \right) + P_r^0 \right) \right) \right]^{-1},$$

$$\Upsilon(x) = \log_2 \left(1 + \frac{(1-x)|\hat{g}_{sr}|^2 p}{(1-x)(pN_{sr} + N_r) + N_{p,r}} \right),$$

$$a = |\hat{g}_{sr}|^2 p + N_r.$$

Proof: Similar to the decode-and-forward relay channel with perfect CSI in [26], f_1 is decreasing, while f_2 and f_3 are increasing in ρ_r . The functions f_2 and f_3 are decreasing and increasing in ρ_d , respectively, while the both functions are decreasing in R_t . So, following the same steps as in Theorem 2 in [26], the optimal solution to (24) is the intersection of the surfaces $R_t = f_1(\rho_r)$, $R_t = f_2(\rho_r, \rho_d, R_t)$ and $R_t = f_3(\rho_r, \rho_d, R_t)$, if exists, otherwise the intersection of the surfaces $R_t = f_1(\rho_r)$, $R_t = f_2(\rho_r, \rho_d, R_t)$ and the plane $\rho_d = 0$ or the intersection of the surface $R_t = f_1(\rho_r)$ and the plane $\rho_r = 0$.

4- Numerical Results and Discussions

In this section the performance of the considered systems is explored numerically. To this end, we consider a setup similar to that of [13] as shown in Fig. 2. It is assumed that there is a line-of-sight path between the source and IRS/relay as well as between the IRS/relay and the destination. Moreover, the channels gains are modeled according to 3GPP Urban Micro (UMi) in [13]. Therefore, the carrier frequency is 3 [GHz], and for line-of-sight channel with distances greater than 10 [m] the channel gain is defined as follows

$$\beta(d) = -37.5 - 22 \log_{10}(d), \quad (30)$$

where d represents the distance between the two node. For the system bandwidth of $B = 10$ [MHz] the noise power is -94 [dBm], and without out loss of generality, the amplitude reflection coefficient is $\alpha = 1$. In addition, processing noise power is assumed to be -84 [dBm] which is typically larger than that of the channel noise. Furthermore, the channel estimation variance is modeled as $N_{sr/rd} = N_e \beta_{sr/rd}$ where $N_e \in [0,1]$ in which $N_e = 1$ are corresponding to perfect channel estimation and useless channel estimation. It is worth

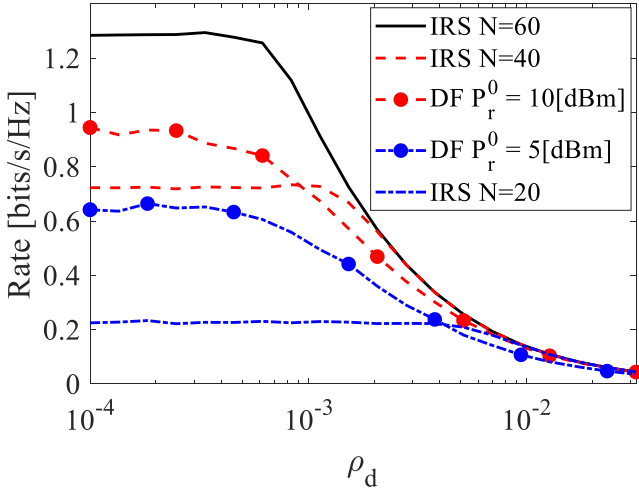


Fig. 3. Achievable data rate versus decoding cost parameter at the destination.

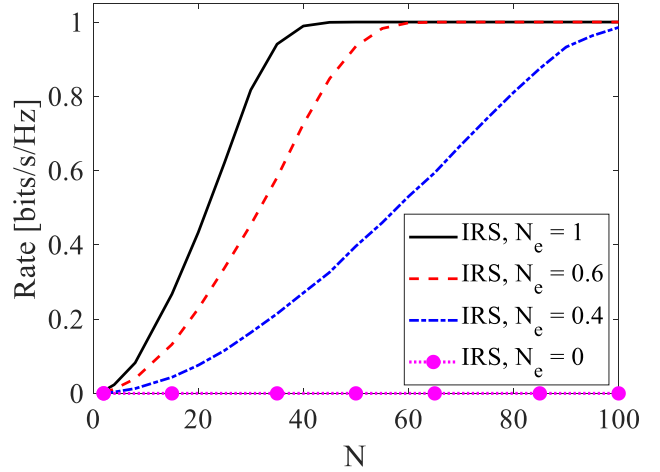


Fig. 6. Achievable data rate versus number of the reflecting element and different channel qualities.

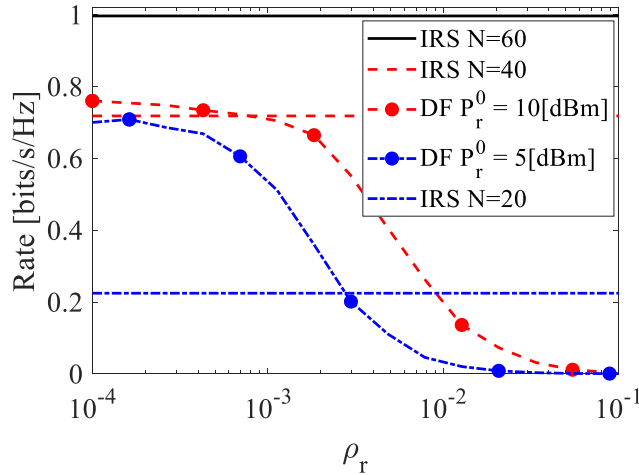


Fig. 4. Achievable data rate versus decoding cost parameter at the relay.

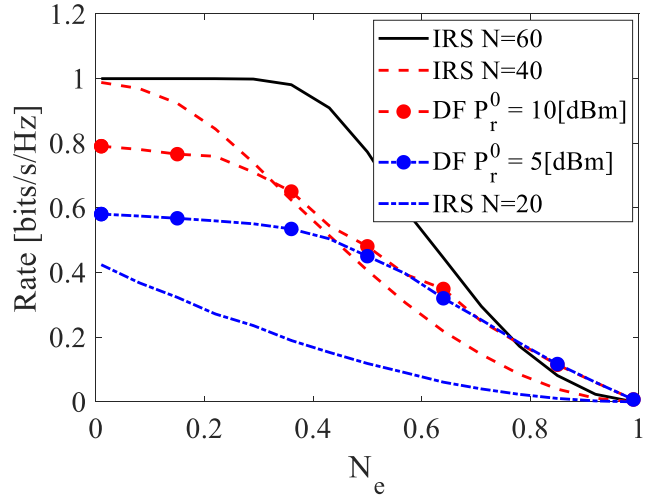


Fig. 7. Achievable data rate versus channel estimation quality.

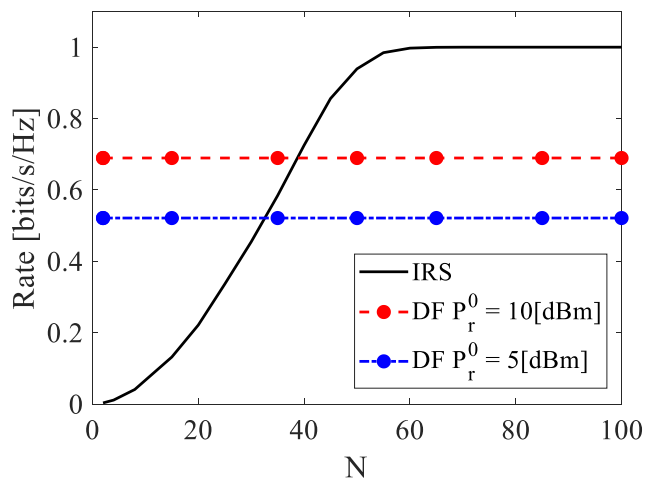


Fig. 5. Achievable data rate versus number of the reflecting elements.

In Fig. 3 data rate of the two systems are shown versus decoding cost parameter at the destination, ρ_d , and it is assumed that $N_e = 0.3$. For smaller number of the reflecting elements relaying scheme outperforms the IRS-assisted transmission; however, as the number of the elements increases IRS-assisted scheme begins to outperform the relaying scenario.

Fig. 4 investigates the impact of the decoding cost at the relay for $N_e = 0.3$. With the increase of ρ_r , more power is required for decoding at the relay and therefore less power remains for retransmission which ultimately leads to lower data rate. Furthermore, for smaller decoding cost at the relay it can outperform the IRS-enabled scenario with small number of reflecting elements.

Figs 5 and 6 depict the data rate versus number of the reflecting elements. In Fig. 5 the data rate of the IRS-assisted transmission is compared with that of the relay-assisted transmission for $P_r^0 = 5$ [dBm] and $P_r^0 = 10$ [dBm] and $N_e = 0.3$. As it is shown in this Fig. by increasing the relay's

noting that the results are averaged over 1000 realizations of the channel coefficients.

inherent power its data rate increases and outperforms the IRS-assisted one; however, as the number of the reflecting elements grows larger than 40 the IRS-assisted transmission becomes advantageous. Furthermore, from Fig. 6 one can see that as the channel estimation quality improves the data rate increases.

Finally, Fig. 7 illustrates the data rate versus variance of the channel estimation error. As we expect as the channel estimation quality reduces the data rate for both IRS- and relay-assisted decreases. This effect for different values of the reflecting elements and relay's inherent power holds and depending on the number of the reflecting element at for different channel estimation qualities IRS-assisted transmission may or may not outperform the relay-assisted one.

5- Conclusions

In this paper, we investigated the impacts of utilizing state-of-the-art IRS in PS-SWIPT-enabled system where imperfect CSI and decoding cost was considered to study a more real world scenario. To understand the advantages of employing IRS, a decode-and-forward relaying scenario was also considered. For both systems the maximum achievable data rates were obtained in the closed-form by optimizing the phase-shift variables in IRS, and power splitting ratio in both systems. Moreover, the result of the IRS was extended to include multiple IRS scenario. Finally, the performance of the systems examined numerically which pointed out that for large enough number of the reflecting elements IRS-assisted transmission outperforms the relay-assisted scenario.

6- References

- [1] E. Björnson, J. Hoydis, L. Sanguinetti, Massive MIMO networks: Spectral, energy, and hardware efficiency, *Foundations and Trends® in Signal Processing*, 11(3-4) (2017) 154-655.
- [2] C. Liaskos, S. Nie, A. Tsioliaridou, A. Pitsillides, S. Ioannidis, I. Akyildiz, A new wireless communication paradigm through software-controlled metasurfaces, *IEEE Communications Magazine*, 56(9) (2018) 162-169.
- [3] E. Björnson, L. Sanguinetti, H. Wymeersch, J. Hoydis, T.L. Marzetta, Massive MIMO is a Reality-What is Next? Five Promising Research Directions for Antenna Arrays, arXiv preprint arXiv:1902.07678, (2019).
- [4] S. Hu, F. Rusek, O. Edfors, Beyond massive MIMO: The potential of data transmission with large intelligent surfaces, *IEEE Transactions on Signal Processing*, 66(10) (2018) 2746-2758.
- [5] Q. Wu, R. Zhang, Towards Smart and Reconfigurable Environment: Intelligent Reflecting Surface Aided Wireless Network, arXiv preprint arXiv:1905.00152, (2019).
- [6] Y.-C. Liang, R. Long, Q. Zhang, J. Chen, H.V. Cheng, H. Guo, Large Intelligent Surface/Antennas (LISA): Making Reflective Radios Smart, arXiv preprint arXiv:1906.06578, (2019).
- [7] C. Huang, G.C. Alexandropoulos, A. Zappone, M. Debbah, C. Yuen, Energy efficient multi-user MISO communication using low resolution large intelligent surfaces, in: 2018 IEEE Globecom Workshops (GC Wkshps), IEEE, 2018, pp. 1-6.
- [8] Q. Wu, R. Zhang, Intelligent reflecting surface enhanced wireless network: Joint active and passive beamforming design, in: 2018 IEEE Global Communications Conference (GLOBECOM), IEEE, 2018, pp. 1-6.
- [9] T.M. Cover, J.A. Thomas, Elements of information theory, John Wiley & Sons, 2012.
- [10] M. Di Renzo, M. Debbah, D.-T. Phan-Huy, A. Zappone, M.-S. Alouini, C. Yuen, V. Sciancalepore, G.C. Alexandropoulos, J. Hoydis, H. Gacanin, Smart radio environments empowered by reconfigurable AI metasurfaces: an idea whose time has come, *EURASIP Journal on Wireless Communications and Networking*, 2019(1) (2019) 129.
- [11] C. Huang, A. Zappone, G.C. Alexandropoulos, M. Debbah, C. Yuen, Large intelligent surfaces for energy efficiency in wireless communication, arXiv preprint arXiv:1810.06934, (2018).
- [12] S. Hu, F. Rusek, O. Edfors, Capacity degradation with modeling hardware impairment in large intelligent surface, in: 2018 IEEE Global Communications Conference (GLOBECOM), IEEE, 2018, pp. 1-6.
- [13] E. Björnson, Ö. Özdogan, E.G. Larsson, Intelligent Reflecting Surface vs. Decode-and-Forward: How Large Surfaces Are Needed to Beat Relaying?, arXiv preprint arXiv:1906.03949, (2019).
- [14] Q. Wu, R. Zhang, Beamforming Optimization for Wireless Network Aided by Intelligent Reflecting Surface with Discrete Phase Shifts, arXiv preprint arXiv:1906.03165, (2019).
- [15] I. Krikidis, S. Timotheou, S. Nikolaou, G. Zheng, D.W.K. Ng, R. Schober, Simultaneous wireless information and power transfer in modern communication systems, *IEEE Communications Magazine*, 52(11) (2014) 104-110.
- [16] C. Peng, F. Li, H. Liu, Optimal power splitting in two-way decode-and-forward relay networks, *IEEE Communications Letters*, 21(9) (2017) 2009-2012.
- [17] H. Liu, K.J. Kim, K.S. Kwak, H.V. Poor, Power splitting-based SWIPT with decode-and-forward full-duplex relaying, *IEEE Transactions on Wireless Communications*, 15(11) (2016) 7561-7577.
- [18] X. Wang, J. Liu, C. Zhai, Wireless power transfer-based multi-pair two-way relaying with massive antennas, *IEEE Transactions on Wireless Communications*, 16(11) (2017) 7672-7684.
- [19] Y. Lou, Y. Zheng, J. Cheng, H. Zhao, Performance of SWIPT-Based Differential AF Relaying Over Nakagami- m Fading Channels With Direct Link, *IEEE Wireless Communications Letters*, 7(1) (2017) 106-109.
- [20] Q. Li, Q. Zhang, J. Qin, Secure relay beamforming for SWIPT in amplify-and-forward two-way relay networks, *IEEE Transactions on Vehicular Technology*, 65(11) (2016) 9006-9019.
- [21] J. Tang, D.K. So, N. Zhao, A. Shojafard, K.-K. Wong, Energy efficiency optimization with SWIPT in MIMO broadcast channels for Internet of Things, *IEEE Internet of Things Journal*, 5(4) (2017) 2605-2619.
- [22] Y. Huang, M. Liu, Y. Liu, Energy-efficient SWIPT in IoT distributed antenna systems, *IEEE Internet of Things Journal*, 5(4) (2018) 2646-2656.
- [23] A. Arafa, S. Ulukus, Optimal policies for wireless networks with energy harvesting transmitters and receivers: Effects of decoding costs, *IEEE Journal on Selected Areas in Communications*, 33(12) (2015) 2611-2625.
- [24] A. Arafa, A. Baknina, S. Ulukus, Energy harvesting two-way channels with decoding and processing costs, *IEEE Transactions on Green Communications and Networking*, 1(1) (2016) 3-16.
- [25] C. Qin, W. Ni, H. Tian, R.P. Liu, Y.J. Guo, Joint beamforming and user selection in multiuser collaborative MIMO SWIPT systems with nonnegligible circuit energy consumption, *IEEE Transactions on Vehicular Technology*, 67(5) (2017) 3909-3923.
- [26] M. Abedi, H. Masoumi, M.J. Emadi, Power splitting-based SWIPT systems with decoding cost, *IEEE Wireless Communications Letters*, (2018).

HOW TO CITE THIS ARTICLE

H. Masoumi, M. J. Emadi, Performance Analysis of cooperative SWIPT System: Intelligent Reflecting Surface versus Decode-and-Forward, *AUT J. Model. Simul.*, 51(2) (2019) 241-248.

DOI: 10.22060/miscj.2019.16626.5165

